

Weak Quantum Ergodicity

L. Kaplan ^{*}

*Department of Physics and Society of Fellows,
Harvard University
Cambridge, Massachusetts 02138*

E. J. Heller[†]

*Department of Physics, Harvard University and
Harvard-Smithsonian Center for Astrophysics
Cambridge, Massachusetts 02138*

(February 5, 2008)

We examine the consequences of classical ergodicity for the localization properties of individual quantum eigenstates in the classical limit. We note that the well known Schnirelman result is a weaker form of quantum ergodicity than the one implied by random matrix theory. This suggests the possibility of systems with non-gaussian random eigenstates which are nonetheless ergodic in the sense of Schnirelman and lead to ergodic transport in the classical limit. These we call “weakly quantum ergodic.” Indeed for a class of “slow ergodic” classical systems, it is found that each eigenstate becomes localized to an ever decreasing fraction of the available state space, in the semiclassical limit. Nevertheless, each eigenstate in this limit covers phase space evenly on any classical scale, and long-time transport properties between individual quantum states remain ergodic due to the diffractive effects which dominate quantum phase space exploration.

I. INTRODUCTION

The issue of quantum correspondence to classical ergodicity has received much attention in recent years. Important questions surround the properties of individual quantum eigenstates of classically ergodic systems. How do eigenstates reflect the ergodic nature of the underlying classical dynamics, in the classical limit? Must they be individually ergodic? What latitude is there in the eigenstates in order that they support classical ergodicity in the correspondence limit? There is a history of interesting conjectures, numerical results, theories, and even theorems in this field. Our focus here is on ergodic systems which are not chaotic in the sense of positive Lyapunov exponents, as these systems spawn the unusual eigenstate properties uncovered in this paper.

A natural place to begin is with two important conjectures. In 1983 Berry suggested that eigenstates of classically ergodic systems locally look like random superpositions of plane waves [1]. Essentially, “random superposition” here means the addition of plane waves with random direction, amplitude, and phase, all having the same local wavelength. The central limit theorem makes it unimportant what distribution the amplitudes are drawn from, as long as they are truly random and independent.

The second landmark conjecture is due to Bohigas, Giannoni, and Schmit [2]. They suggested that spectra (and eigenstate properties) of classically chaotic Hamiltonian systems would be identical to those of random matrix theory (RMT) [3] (see also Ref. [4]) in the classical limit. This implies strong level repulsion in the spectrum and Gaussian random eigenfunctions, with detailed characteristics of both varying according to symmetry properties of the system (e.g. the presence or absence of time reversal symmetry).

Subsequent numerical and theoretical work has borne out these conjectures in large part, with modifications that can be ascribed to short time classical dynamics. Classical chaos in the presence of a typical Lyapunov exponent $\bar{\lambda} > 0$ takes on the order of the “log time,” $t = |\log \hbar|/\bar{\lambda}$, to spread a Planck-sized cell everywhere allowable in phase space on a Planck-scale mesh (at which time the cell has lost all memory of its initial location) [5]. This is associated with the positive entropy of the chaotic dynamics, which destroys the information contained in the initial wavepacket. Following the log-time the classical dynamics begins to create structures in phase-space on sub-Planck scales, which get washed out quantum mechanically by the uncertainty principle. Before this time, the imprint of nonrandom classical mechanics is written or encoded into the quantum mechanics, so to speak. Time dependent semiclassical approximations hold for a time at least on the order of the log time [5]. Since the quantum eigenstates

^{*}kaplan@physics.harvard.edu

[†]heller@physics.harvard.edu

(and their eigenvalues) support the short-time as well as the long-time dynamics, they must possess corrections to RMT. However, since it takes a much longer time (the Heisenberg time, or $\hbar/\delta E$, where δE is the mean level spacing) to resolve individual eigenstates, the corrections to universal RMT behavior often involve collective properties of many nearby eigenvalues and their corresponding eigenstates.

These corrections stand out against the monotonous backdrop of RMT. For example, some eigenstates have enhanced amplitude near, i.e. are “scarred” by, certain short isolated unstable periodic orbits. Although random eigenstates (in the sense of Berry’s conjecture) have scar-like concentrations when viewed in coordinate space [6], eigenstates of chaotic systems have scars associated with definite periodic orbits [7]. The theory of scars [7–9] depends only on short time, linearized dynamics near the periodic orbit. These are “linear” scar theories, they do not tell us *which* states are scarred or what individual states look like. Nonlinear scar theories provide information about how scar density from a given orbit is distributed among individual eigenstates [10]; these theories are still under development [11].

Other corrections to RMT involve nonuniversal correlations in eigenvalue spectra, which also arise from short periodic orbits [12]. Much numerical evidence supports the existence of scars and nonuniversal spectral correlations.

Given that deviations from RMT are known to exist, the question arises as to how strong a form of quantum ergodicity is actually required for a system which is classically ergodic. Naively, classical–quantum correspondence only has implications for properties averaged over many eigenstates, such as transport efficiency from one region of phase space to another. What are the constraints imposed on individual eigenstates?

A very important result in this regard was proved by Schnirelman [13] and Colin de Verdiere [14] (see also Zelditch [15]). The result states that in the classical limit, the quantum expectation value of certain operators¹ over *individual* eigenstates is almost always the ergodic, microcanonical average of the classical version of the operator, proving the ergodicity of individual eigenstates on a “macroscopic” scale. Colin de Verdiere’s proof left a loophole for a possible measure zero set of states which could violate ergodicity; he conjectured however that the exceptions did not exist. It was shown later that a strongly phase space localized (but zero measure as $\hbar \rightarrow 0$) set of states could indeed exist [17]. In effect, Schnirelman–Colin de Verdiere–Zelditch (SCdVZ) showed that eigenstates of classically ergodic systems cannot deviate from ergodicity when smoothed over any finite patch of phase space as $\hbar \rightarrow 0$. Importantly, the presence of macroscopic, classical scale ergodicity leaves open the question of microscopic ergodicity, on classically infinitesimal (but quantum mechanically large) scales.

An example of a possible “microscopic” scale is a length scaling as $\sqrt{\hbar}$. This length, although becoming (as $\hbar \rightarrow 0$) insignificant on any scale over which a smooth classically-defined operator can vary, contains infinitely many de Broglie wavelengths in the same limit. One might suppose that eigenstates of classically chaotic systems are generally ergodic even on these microscopic scales, but this remains to be shown. Eigenstates behaving in accordance with RMT would be microscopically ergodic, forbidding large deviations in $|\psi|^2$ when averaged over a $\sqrt{\hbar}$ length scale (or indeed over any scale large compared to \hbar) as $\hbar \rightarrow 0$. To put it another way, *random matrix theory is a far more stringent requirement than SCdVZ ergodicity*. It seems appropriate to call SCdVZ “weak quantum ergodicity”: eigenfunctions which are not Gaussian random in most representations can still be ergodic in the sense of SCdVZ. A weakly quantum ergodic eigenstate can become localized to an ever decreasing fraction of the available state space, in the classical limit, but in such a way that the coarse graining provided by taking the expectation value of any classically smooth operator leads to a result which is not anomalous. This paper shows that the regime of weak quantum ergodicity exists, and provides examples.

We first develop a general formalism for analyzing and comparing various types of localization phenomena. Then the implications of classical ergodicity for the properties of quantum eigenstates and quantum transport are discussed, and compared with random matrix theory (RMT) predictions. Several known examples of anomalous (non-RMT) behavior in classically ergodic systems are mentioned. It is shown how such anomalies (and indeed even more striking ones) are consistent with the predictions of Schnirelman–Colin de Verdiere. We examine the important effect that classical spreading rates have on quantum behavior, and on the relative importance of classical and diffractive phase space exploration. Finally, we discuss two examples of weakly quantum ergodic systems.

¹Specifically, Colin de Verdiere’s proof deals with pseudo-differential operators, acting on eigenstates of the Laplacian on a compact space without boundaries. Zelditch’s work extends these results to billiards with piecewise smooth walls, with the condition that the kernel of the operator must be supported away from the walls. Others have dealt with the case of a compact classical phase space [16].

II. LOCALIZED EIGENSTATES AND ERGODIC QUANTUM TRANSPORT

The question of quantum ergodicity for conservative Hamiltonian systems suffers from the following conceptual problem: energy is conserved in both classical and quantum mechanics, and is a known *a priori* constraint on the dynamics. In classical mechanics this is easily handled by considering ergodicity on the energy hypersurface; in quantum mechanics it would beg the question to do so, since the only states with fixed energy are eigenstates. These are unique unless the spectrum is degenerate. Thus, if we insist on working on an energy hypersurface, all nondegenerate systems are trivially ergodic. This in fact was the basis of von Neumann's approach to quantum ergodicity. It has the problem of an absence of classical-quantum correspondence for nondegenerate systems. The problem is resolved by considering flow between phase space localized states (usually coherent states) [18]. These of course populate a range of energies, but the moments of the energy distribution for any such state are known from very short time dynamics. Then it is straightforward to develop criteria for ergodic flow between such localized states [18].

If energy is not conserved (as in a kicked system) the problem of incorporating the *a priori* constant energy constraints does not arise². The situation is also conceptually simpler in any space where for some reason each basis state is *a priori* equally accessible. An example is a kicked symmetric top where the kick preserves total angular momentum J and body-axis angular momentum K (and thus the energy) but not M , the space fixed z -component of angular momentum. Then all $(2J+1)$ M states are degenerate and are equal candidates for flow under the dynamics. The semiclassical limit is $J \rightarrow \infty$. Every M state in the space can be made equally accessible starting from any other state, or any superposition of states. We will formulate the transport theory and our models along these lines, but weakly quantum ergodic systems will exist more generally, even in the presence of constraints imposed by classical symmetries.

The problem of localization *vs.* ergodicity may be stated as the problem of the distribution of overlap probabilities

$$p_n^a = |\langle a | n \rangle|^2 \equiv |\alpha_n^a|^2, \quad (1)$$

where $|a\rangle$ is some physically appropriate basis spanning an eligible subspace, and $|n\rangle$ are eigenstates of the propagator (e.g. a kick) spanning the same space. “Eligible” means states that are accessible to the dynamics according to all *a priori* constraints. The probabilities are normalized, i.e.

$$\sum_n p_n^a = \sum_a p_n^a = 1. \quad (2)$$

If the propagator is a discrete quantum unitary map S , the eigenstates $|n\rangle$ are specified by

$$S|n\rangle = e^{i\phi_n}|n\rangle, \quad (3)$$

where the real phase ϕ_n puts all the eigenvalues on the unit circle. If the total Hamiltonian can be written as $H = H_0 + \delta H$, it may be interesting to use the eigenstates of H_0 as the basis $|a\rangle$, and to consider how these are intermixed by the perturbation δH . For example, for a particle hopping on a random lattice, as in the case of Anderson localization, the position basis may be a natural one to use. There we can imagine starting with random on-site potentials and adding nearest-neighbor couplings as a perturbation. In the scattering and kicked systems discussed towards the end of this paper, we will take the reference basis $|a\rangle$ to be momentum eigenstates (or channels in the case of scattering). Other bases, such as phase space bases, may also be important in various contexts (e.g. in the presence of constraints imposed by time translation invariance or other symmetries).

Under discrete time dynamics, governed by a unitary operator S , a state $|a\rangle$ becomes after ℓ iterations

$$|a_\ell\rangle = S^\ell|a\rangle = \sum_n \exp[i\ell\phi_n]\alpha_n^a|n\rangle, \quad (4)$$

so that in the nondegenerate case the time averaged density corresponding to the initial state $|a\rangle$ becomes

² Of course any non-autonomous system is equivalent to an autonomous one in an extended phase space. In this extended phase space, the ergodic dynamics would only produce uniform coverage on the constant-“energy” hypersurface, as discussed in the preceding paragraph.

$$\begin{aligned}
\rho_a^\infty &\equiv \lim_{L \rightarrow \infty} \frac{1}{L} \sum_{\ell=1}^L \sum_{n,n'} |n\rangle \langle n|a\rangle \langle a|n'\rangle \langle n'| \exp[-i\ell(\phi_{n'} - \phi_n)] \alpha_n^a (\alpha_{n'}^a)^* \\
&= \sum_n p_n^a |n\rangle \langle n|.
\end{aligned} \tag{5}$$

Time averaged flow from state $|a\rangle$ to $|b\rangle$ (or *vice-versa*) is governed by the p_n^a (for the nondegenerate case) as

$$P(a|b) = \lim_{L \rightarrow \infty} \frac{1}{L} \sum_{\ell=1}^L |\langle a|S^\ell|b\rangle|^2 = \sum_{n=1}^N p_n^a p_n^b. \tag{6}$$

A. Strong ergodicity

A form of ergodicity which is too strict follows if we insist that $P(a|b) = 1/N$ for all a and b , in the semiclassical limit. (Note that in this limit N , the dimension of the Hilbert space, goes to infinity.) No variation is permitted in the p_n^a 's: the condition $p_n^a = 1/N$ is necessary under such “strict ergodicity”, else e.g. $P(a|a) > P(a|b)$ for $b \neq a$. Even “random” eigenstates with Gaussian random fluctuations in α_n^a fail strict quantum ergodicity. We therefore retreat to define *strong quantum ergodicity* to mean p_n^a given by RMT: p_n^a 's must be given by a χ^2 distribution of one or two degrees of freedom, depending on whether α_n^a is real or complex, respectively.

$P(a|b)$ is a quantum state-to-state measure of long-time transport. Transport involving operators must also be considered. The trace of an operator F is defined as

$$\text{Tr}F = \frac{1}{N} \sum_b \langle b|F|b\rangle. \tag{7}$$

For F diagonal in the physically-motivated basis $|a\rangle$, $F = \sum_a |a\rangle f(a)\langle a|$. A time average of F results in

$$\bar{F} = \sum_n \sum_a |n\rangle p_n^a f(a) \langle n| = \sum_n f_n |n\rangle \langle n|, \tag{8}$$

with

$$f_n \equiv \sum_a p_n^a f(a) = \langle n|F|n\rangle. \tag{9}$$

Strict ergodicity is equivalent to assuming

$$f_n \rightarrow \text{Tr}(F), \tag{10}$$

independent of n , for arbitrary F , as $N \rightarrow \infty$. In other words, the time average of F must be evenly distributed over the entire available space. (This requires $p_n^a \rightarrow 1/N$, since $f(a)$ is arbitrary. An example is $F = \sum_{a' \in A} |a'\rangle \langle a'|$ where A is some set of states.) If we put some restrictions on F , so that the $f(a)$ are sufficiently distributed over many states a , then strong ergodicity is sufficient to ensure Eq. (10) holds. An example is for a to be the position basis, with $f(a)$ spread over a range of lengths of the order of $\sqrt{\hbar}$.

B. Weak ergodicity

The concept of weak ergodicity applies to further restricted operators F , namely those which correspond to classical symbols. Weak ergodicity exploits the fact that a classically defined F must have smooth variation of $f(a)$ with a , as $N \rightarrow \infty$, over macroscopic ranges. Given weak quantum ergodicity, Eq. (10) still holds, with the macroscopic smoothness restriction on $f(a)$. The smoothness of $f(a)$ places much less demand on the individual p_n^a 's. They need only average to uniformity over macroscopic regions. This leaves considerable latitude for the microscopic behavior of the p_n^a . We conjecture that the underlying classical dynamics will determine the statistical properties of non-RMT p_n^a .

Weak ergodicity corresponds to SCdVZ: (almost) every stationary state is individually ergodic when measured over a smooth macroscopic classical distribution, i.e. $\langle n|F|n\rangle = f_n \rightarrow \text{Tr}(F)$ for smooth F in the semiclassical limit.

RMT on the other hand implies that each p_n^a should behave as an absolute square of an independent Gaussian variable, giving as non-trivial results

$$\langle P(a|b)^2 \rangle = \frac{1}{N^2}; \quad \langle P(a|a) \rangle = \frac{s}{N}, \quad (11)$$

where $P(a|a)$ (a time-averaged autocorrelation function for non-degenerate spectra) is the diagonal part of the $P(a|b)$ matrix, and s takes the value of 2 for generic hermitian Hamiltonians or real Hamiltonians with complex states $|a\rangle$ (GUE statistics), and 3 for real symmetric Hamiltonians with real states $|a\rangle$ (GOE statistics, appropriate for time-reversal invariant systems). The measure $\mathcal{F} = 1/(N \langle P(a|a) \rangle)$ is the fraction of the eligible eigenstates with which a typical state has significant overlap [18]. The averages in Equation (11) are taken over all states, as well as over an appropriate ensemble of systems. $\langle P(a|a) \rangle$, in addition to being a long-time averaged autocorrelation function, also measures the first non-trivial moment of the p_n^a distribution. $\mathcal{P} = \langle P(a|b)^2 \rangle$ measures state-to-state transport fluctuations, at long times. An eigenstate-specific statistic can also be defined:

$$P(n|n) = \sum_a (p_n^a)^2, \quad (12)$$

which measures the inverse participation ratio for that eigenstate, that is, the inverse of the number of states $|a\rangle$ with which the eigenstate $|n\rangle$ has substantial overlap. The mean of the $P(n|n)$ distribution is obviously equal to that of $P(a|a)$. Thus, RMT implies (up to a factor of 2 or 3 arising from quantum fluctuations) ergodicity of eigenstates projected onto individual quantum states, as measured by \mathcal{F} (as well as ergodic transport at the single-state level, as measured by \mathcal{P} , which, as will be shown explicitly later on, is in fact a weaker condition). In this paper, deviations from single-state ergodicity are examined which are still consistent with the state-averaged Schnirelman results.

III. EXAMPLES OF LOCALIZATION

We will briefly discuss a few known examples of localization phenomena, putting them in the language presented above. By “localization” here is meant an anomalously large expectation value $N \langle P(a|a) \rangle$ or $N^2 \langle P(a|b)^2 \rangle$, compared with the RMT predictions. Examples include scarring, weak localization, and dynamical localization. Most of these localization phenomena disappear or become much less important as $\hbar \rightarrow 0$. The effects we study here become *increasingly dramatic* as $\hbar \rightarrow 0$.

Scarring is an enhancement of the return probability $P(a|a)$ associated with an unstable periodic orbit in the corresponding classical system. It is a striking example of the influence of short-time classical dynamics on long-time quantum properties in classically chaotic systems. It can be shown by semiclassical arguments (and assuming randomness in the homoclinic tangle associated with the periodic orbit), that there is a universal scarring enhancement factor $\alpha(\lambda)$ for an initial state lying on an unstable periodic orbit with exponent λ . Thus, when averaging over an appropriate ensemble,

$$\langle P(a|a) \rangle = \frac{\alpha(\lambda)s}{N}, \quad (13)$$

where $\alpha(\lambda)$ is a function that decreases to 1 as $\lambda \rightarrow \infty$, s is the RMT quantum fluctuation factor mentioned above, and $|a\rangle$ is a coherent state centered on a periodic point. However, significant enhancement is found only for those initial states $|a\rangle$ which lie close to a periodic orbit with a small amount of instability, and these comprise a vanishing fraction of the total state space in the semiclassical limit. Thus quantities such as $\langle \sum_a P(a|a) \rangle$ will still be generic as $\hbar \rightarrow 0$.

Weak localization is a (factor of 2) backscattering enhancement in time-reversal invariant systems which can be understood semiclassically as resulting from the constructive interference between any given returning path and its time-reversed image. This enhancement factor is a constant over all incoming states, is preserved as $\hbar \rightarrow 0$, and gives rise to a corresponding enhancement in the inverse participation ratios $P(n|n)$ of the S-matrix eigenstates.

Finite enhancement factors for selected $P(a|a)$ are also found in systems with a discrete symmetry group. Anomalous autocorrelation statistics arise for initial states which are eigenstates of the relevant symmetry transformation. This effect can combine with scarring to produce more eigenstate localization in symmetric chaotic systems such as the stadium billiard than would be expected based on scarring arguments alone [10].

Finally, dynamical localization is a strong localization effect in the sense that it can produce arbitrarily large enhancement of the $\langle P(a|a) \rangle$ (and also of the $\langle P(a|b)^2 \rangle$) statistics, for a given value of Planck’s constant \hbar . So, for example, the quantum kicked rotor (standard map) allows classical diffusion to infinite momenta for

sufficiently large values of the kicking parameter, but the quantum eigenstates remain localized in momentum space. The localization however does not survive the $h \rightarrow 0$ limit, in the sense that the localization length becomes infinite.

The “slow ergodic” systems considered towards the end of this paper present a new phenomenon not present in any of the localization examples given above, in that the eigenstates become *more and more localized* (in the sense of a diverging $N < P(a|a) >$ statistic), as $h \rightarrow 0$. However, the $N^2 < P(a|b)^2 >$ eigenstate-averaged transport statistic seems to converge to a constant in this limit. Before describing the detailed properties of these unusual quantum systems, it is shown how such anomalies are mathematically possible in the formalism outlined above.

IV. FAILING STRONG ERGODICITY

Since the Schnirelman test effectively averages eigenstates in the semiclassical limit over a finite region in the classical phase space (which includes infinitely many wavelengths in this limit), it is not necessary for eigenstate ergodicity to obtain at scales of the order of Planck’s constant. In fact, for eigenstates to be ergodic on a classically fixed mesh as $N \rightarrow \infty$, it is sufficient for the number of states in which a typical eigenstate lives (the inverse of the $< P(a|a) >$ statistic) to be an increasing function of N , provided the $1/ < P(a|a) >$ states are spread evenly enough over the classical phase space. There is no requirement for $1/ < P(a|a) >$ to be a linear function of N . Notice that if this function is slower than linear, the eigenstates become less and less ergodic at the individual state level as $h \rightarrow 0$ ($N \rightarrow \infty$), even as they appear more and more smooth on classical scales.

What about the transport statistic $N^2 < P(a|b)^2 >$? Assuming the elements p_n^a are statistically independent (but not necessarily Gaussian) variables gives the following relationship between $N^2 < P(a|b)^2 >$ and $N < P(a|a) >$:

$$\begin{aligned} N^2 < P(a|b)^2 > &= 1 + \frac{2}{N} (N < P(a|a) >)^2 + \frac{1}{N^2} < N^4 (p_n^a)^4 > \\ &\equiv C_1 + C_2 (N < P(a|a) >)^2 + C_3 < N^4 (p_n^a)^4 >. \end{aligned} \quad (14)$$

(Recall that $N < P(a|a) >$ measures the second moment of the p_n^a distribution.) The second term arises from the $a = b$ and $n = n'$ contributions to the sum on the left hand side. It is apparent that $N^2 < P(a|b)^2 >$ is forced to become anomalous if $N < P(a|a) >$ grows faster than $N^{1/2}$. On the other hand, if $N < P(a|a) > \leq O(N^{1/2})$, then the anomalous nature of the individual eigenstates need not qualitatively affect the transport properties of the system, even at the single-state level. This is a key point of this paper.

In reality, there will always be non-trivial correlations $< p_n^a p_{n'}^b >$ in the eigenstate matrix for $|a\rangle$ and $|b\rangle$ connected by short classical paths, as well as generally for $|a\rangle$ close to $|b\rangle$ (because of diffractive effects). Such classical and quantum spreading tends to increase C_2 in Eq. (14), imposing more stringent limits on the behavior of $N < P(a|a) >$ which is consistent with single-state transport remaining ergodic³. Non-trivial classical and diffractive transport characteristics can also change C_1 in Eq. (14) from the RMT prediction of 1. This, however, is a less dramatic form of localization, because this deviation from RMT predictions does not become ever more pronounced in the semiclassical limit.

V. CLASSICAL ERGODICITY

Classical ergodicity (time average equals phase space average) implies that each phase-space ball of radius ϵ ⁴ should evenly cover all of phase space under the dynamics, thus intersecting every other ball of the same radius after being evolved for a sufficiently long time. One may ask how the time T required to achieve this uniform coverage scales with ϵ . This allows for a hierarchy within the class of ergodic systems. For a purely mixing (chaotic) system, such as the baker’s map or the stadium billiard, T scales logarithmically with ϵ ; in other words, after a finite time, phase space has been explored on an exponentially fine scale. For an ergodic system with zero Lyapunov exponent, T and ϵ are related by a power law (the power may depend on the basis under consideration, as well as on the details of the system). Examples of such systems include generic polygonal two-dimensional billiards, and kicked one-dimensional

³It is intuitively clear that increasing the amount of transport in the classical system cannot make quantum transport *less* ergodic – it can, however, make the eigenstates *more* ergodic, *i.e.* less anomalous.

⁴Or an x- or p-strip of width ϵ . The rates of spreading may well be different in different coordinates, so that quantum ergodic properties are sensitive to the choice of basis.

systems with piecewise-linear periodic potentials. A “slow ergodic” system is one for which T scales exponentially with ϵ – for this class of systems it takes an exponentially long time to explore phase space evenly on a mesh of a given scale. This will have profound consequences for the quantum versions of these systems, in that the number of states classically accessed by the Heisenberg time (which is a natural cutoff time for the quantum mechanics) can be a small fraction of the total number of available states, even though the system is classically ergodic.

This behavior is in stark contrast with mixing systems, in which an exponentially large number of classical paths connect any two quantum states by the Heisenberg time. In mixing systems, interference effects have to work against classical spreading to produce deviations from RMT behavior⁵. Such interference produces the weak localization and “discrete symmetry” localization effects described in a previous section, but it only leads to at most a factor of order 1 deviation from RMT predictions. This line of argument also suggests that diffraction may be less important in hard chaotic systems than in non-mixing systems, because semiclassical dynamics already produces very efficient wavepacket spreading and transport, helping to explain why semiclassical methods do such a surprisingly good job of reproducing quantum mechanical spectra and eigenstates in systems like the baker’s map.

In the “slow ergodic” systems, on the other hand, only a very small number of states are accessed classically by the Heisenberg time, so the non-classical effects (diffraction, in particular), are essential to understanding even qualitatively the quantum mechanical properties of these systems at the single-state level. These systems may well prove to be the best examples of non-universal quantum ergodic behavior.

In “ordinary ergodic” systems, characterized by a power-law spreading rate, the situation is intermediate between these two extremes. In such systems, there may be either of order 1 or a power of N (depending on the system as well as on the basis chosen) classical paths leading from a given state to any other state by the Heisenberg time. The effectiveness of semiclassical methods (as well as the validity of RMT predictions) is expected to be intermediate between the cases described above.

VI. EXAMPLES

A. Tilted Billiard

The first example of a “slow ergodic” system is the “tilted billiard,” constructed by taking a corridor formed by two horizontal walls (in two dimensions) a distance 2π apart, and closing off the right end with a wall segment placed at some (small) angle α to the vertical, the other end being left open (for now). A classical particle, sent in from the left end at an angle θ from the horizontal, hits the tilted wall, returning at a new angle θ' (see Fig. (1)).

For angles θ' far from the vertical, θ' is (up to a minus sign) given by $\theta \pm 2\alpha$, depending on whether the billiard hits the tilted wall from above or below. Near the vertical, a double bounce off of the tilted wall can lead to $|\theta'| = \theta \pm 4\alpha$. The angle can always be taken to be in the first or fourth quadrant; then the double bounce allows the motion in angle space to “wrap around” from $\theta = \pi/2 - \epsilon$ to $\theta' = -\pi/2 + 4\alpha - \epsilon$ (for $\alpha < \epsilon < 3\alpha$), and similarly in the other direction.

Now a vertical wall can be set up on the left at a distance d from the tilted wall, so that the process of bouncing off the tilted wall is iterated (consider a surface of section map, taking the surface to be the left wall). Then for irrational α/π , all values of θ will be accessed eventually for a generic initial condition. We find, however, that the motion in θ -space is *not* a random walk, which would be the case if the probabilities of the billiard ball hitting the tilted wall from above or below were independent of hits on previous iterations. Instead, strong correlations exist, producing “bottlenecks” at certain values θ for any given d . Near these bottlenecks, the particle is much more likely to hit the tilted wall from below if it hit the wall from above on the previous iteration, and vice versa.

FIG. 1. Tilted billiard and definition of angles.

The net result is that the number of angles visited after T lengthwise traversals of the billiard scales only as $\log(T)$, in contrast to \sqrt{T} , which would be the consequence of a random walk process. Similarly, the probability of returning to a given angle after T iterations, scales as $1/\log(T)$. Specifically, if the typical number of angles visited (averaged over an ensemble of values for d and α , and also over initial conditions) is taken to be n_T , and the inverse of the average probability of returning to a given angle is denoted by m_T , then we find

⁵“Hard quantum” effects such as diffraction and tunneling generically will only *add* to the rate of spreading.

$$\begin{aligned} n_T &= r + s \log(T) \\ m_T &= r' + s' \log(T), \end{aligned} \tag{15}$$

with a numerical fit to $m_T = 1.65 + 0.8 \log(T)$ and $n_T = 1.95 + 0.55 \log(T)$, which works for T ranging at least up to 100000 scattering events. For the numerical calculation, we use an ensemble of billiards with billiard length d ranging from 10π to 20π , and tilt angle α between $\pi/20$ and $\pi/10$. For each billiard configuration, an average over starting points is performed.

This system is quantized, and we find (numerically) the S-matrix (at a given energy) for right-moving waves starting at the left end of the billiard colliding with the tilted wall. The states which label the S-matrix are as usual channels characterized by the “asymptotic” eigenmodes in the parallel-wall corridor, i.e.

$$\psi_n(y) = \sqrt{\frac{2}{\pi}} \sin(ny),$$

$n = 1, 2, \dots$. For a rectangular billiard ($\alpha = 0$), the S-matrix is diagonal; for non-zero α , a band-diagonal structure is present, the width of the band being a fraction of order α of the total number of states (Fig. (2)). Classically, the n^{th} scattering channel corresponds to two incoming angles, $\pm\theta_n$, where

$$\theta_n = \tan^{-1} \left[\frac{n}{\sqrt{8E - n^2}} \right].$$

FIG. 2. The S-matrix (absolute value of the 96×96 matrix) for $d = 2\pi$, $\alpha = \pi/36.3777$, and $E = 1120.85$ ($m = \hbar = 1$).

In particular, if the phases of the incoming and outgoing plane waves are fixed, by fixing the billiard length d , we can diagonalize the S-matrix and consider the properties of the S-matrix eigenstates. Eigenstates with eigenvalue -1 are in fact also eigenstates of the closed billiard; other S-matrix eigenstates correspond to unusual boundary conditions in the closed system, where the wave acquires an arbitrary phase upon bouncing off of the vertical wall. This is actually a way of finding eigenvalues and eigenstates of the billiard with Dirichlet boundary conditions; they are given by eigenstates of S with eigenvalue -1 [19,20]. However here we do not seek the Dirichlet solutions, since they are not special as far as their localization in the channel space (this has been tested numerically). Two typical S-matrix eigenstates are shown in Fig. (3); these show fairly obvious non-statistical mixing of different directions of propagation in the billiard (nonmixing of channels in the scattering approach).

FIG. 3. Showing two typical S-matrix eigenstates for the parameters given in Fig. (2).

Hitting the wall with positive θ results in the next hit being at two possible angles, namely $\pm(\theta + 2\alpha)$; hitting the wall with negative θ results in the next hit also being at two possible angles, namely $\pm(\theta - 2\alpha)$. Each channel scatters to the vicinity of two new channels, usually one with higher angles and one with lower angles of approach to the tilted wall. (The exceptions are at extreme values of the angle, near 0 and $\pm\pi/2$. For example at low incident angle (low n) the new classically-accessible channels are both higher in angle). The S and the $P(a|b)$ matrices in the channel basis display properties stemming from the classical behavior of this system. In particular, S (see Fig. (2)) shows the classical imprint of the once iterated collision. Figure (4) shows the iterations of S , ending in the time-averaged $P(a|b)$ matrix at the lower right. A detail of $P(a|b)$ is shown in Fig. (5).

FIG. 4. Showing the iterations of S (absolute value of S displayed as density); the $P(a|b)$ matrix is shown at the lower right, for the parameters given in Fig. (2).

FIG. 5. Detail of the $P(a|b)$ matrix, for the parameters given in Fig. (2).

The bands in S (Fig. (2)) are not one but two or three channels wide, falling off more rapidly from there. Typically (for generic d , α , and energy E), $P(a|b)$ has of order $\log(N)$ strong bands approximately parallel and in some places

perpendicular to the diagonal, corresponding to the number of angles classically accessible, in accordance with Eq. (15), by the Heisenberg time (which scales linearly with N). If all the strength were concentrated in these diagonal lines, then both $N < P(a|a) >$ and $N^2 < P(a|b)^2 >$ would increase as $N/\log(N)$ in the classical limit, giving rise to strong localization. This semiclassical prediction is modified, however, due to the presence of diffractive effects. The main source of diffraction in this system follows a roughly power-law behavior away from the classically allowed states,

$$P(a|b) \sim \frac{c_\beta}{Nn} \sum_{j=1}^n \left(\frac{N}{b-j} \right)^\beta , \quad (16)$$

where j runs over states classically accessible from a by the Heisenberg time, n is the number of such states (it scales as $\log(N)$ in the “slow ergodic” systems under consideration), and β is an exponent. Because the diffractive pattern is scale-invariant, $N^2 < P(a|b)^2 >$ is an N -independent constant, though $\beta \leq 1/2$ is required for this second moment to be normalizable. Thus, this measure of single-state long-time transport is only off by a constant from the RMT prediction. In fact, because of diffraction, $N^2 < P(a|b)^2 >$ will not grow linearly with N even in a classically nonergodic version of this system, where the tilt angle is taken to be rational (so that only a finite number of angles are classically accessible). $N < P(a|a) >$, on the other hand, exhibits a growth consistent with $\sqrt{N}/\log(\nu N)$ (corresponding to $\beta = 1/2$ above). The inverse participation ratio $N < P(a|a) >$ would scale as \sqrt{N} in the case of a rational tilt angle, where the logarithmic classical spreading is absent.

FIG. 6. Fit to the form given in Eq. (17).

In Fig. (6), a fit to this form is given. For an ensemble consisting of 30 tilted wall billiards (using three angles $\theta = 0.0692, 0.0759, 0.0845$, and ten lengths spaced equally from $2\pi - 4/5$ to $2\pi + 1$) the $N < P(a|a) >$ measure is shown as a function of the number of channels, from 9 channels to about 160. The data fit the form

$$N < P(a|a) > = \frac{b_1 \sqrt{N}}{b_2 + \log N} \quad (17)$$

very nicely, with $b_1 = 2.87$ and $b_2 = -0.676$. We find that the transport $N^2 < P(a|b)^2 >$ approaches a value of about 3 in the high energy range, which is consistent with ergodic transport. This is an example of a system whose existence was hypothesized earlier, with ergodic (up to a constant) transport, but very non-ergodic individual eigenstates, in the semiclassical limit.

Another source of diffraction causes diffusion of the quantum amplitude: diffraction coming from the corners. A sharp corner is scale invariant, so a given amount of diffracted amplitude emanates from the corner at each iteration as if it were nearly a point source, independent of $N \sim \sqrt{8E}$. This sprays amplitude $\sim \gamma/N$ into each channel, where γ is some small number. As $N \rightarrow \infty$, the total corner diffracted probability scales as $\sum_{n=1}^N \gamma^2 N^{-2} = \gamma^2/N$ at each iteration. Since there are N iterations to the Heisenberg time, and assuming random phases at each iteration, we have $\sqrt{N}\gamma/N$ amplitude in each state due to corner diffraction at the Heisenberg time, or a probability averaging γ^2/N . If this were the only source of flow between channels the result would be localization in channel space for small $\gamma < 1$ (in practice $\gamma \ll 1$); then $N < P(a|a) > \sim N$ and the transport would be anomalous, as discussed above. The power law channel diffraction discussed above dominates the corner diffraction.

B. Sawtooth map

A simple example of a “slow ergodic” system exists also within the domain of (time-dependent) one-dimensional models. The classical kicked sawtooth potential (KSP) map is a discrete-time area-preserving map of the plane onto itself, defined as follows:

$$p' = p + a, \quad x \bmod 1 < 1/2 \quad (18)$$

$$p - a, \quad x \bmod 1 > 1/2 \quad (19)$$

$$x' = x + bp'. \quad (20)$$

Here a is the kicking strength, while b measures the free evolution time between kicks (where the mass is set to 1). We call this a sawtooth potential map⁶ because the evolution in momentum can be re-written as

$$p' = p - V'(x)\Delta t, \quad (21)$$

where $V(x)$ is a periodic sawtooth potential

$$V(x) = -\frac{a}{\Delta t}(x \bmod 1), \quad x \bmod 1 < 1/2 \quad (22)$$

$$\frac{a}{\Delta t}(x \bmod 1 - 1), \quad x \bmod 1 > 1/2, \quad (23)$$

which is turned on for an infinitesimal time Δt , and where the limit $\Delta t \rightarrow 0$ is taken. We will want to compactify this map onto a torus so as to be able to quantize it later using a finite-dimensional Hilbert space. We obtain an area-preserving map of the unit square onto itself⁷

$$p' = (p + a) \bmod 1, \quad x < 1/2 \quad (24)$$

$$(p - a) \bmod 1, \quad x > 1/2 \quad (25)$$

$$x' = (x + bp') \bmod 1. \quad (26)$$

This system can be quantized in the usual way, the discrete quantum time evolution being given by the unitary operator

$$U = e^{-iW(\hat{p})/\hbar} e^{-iV(\hat{x})/\hbar} \quad (27)$$

where $W(p)$ is a kinetic term given by

$$W(p) = -\frac{1}{2}b(p \bmod 1)^2 \quad (28)$$

Note that if $b = 1$, then equivalently we may take $W(p) = -\frac{1}{2}bp^2$. This would result in a different quantization corresponding to the same classical dynamics.

When quantizing evolution on a torus, a choice of boundary conditions needs to be made. Periodic boundary conditions are most natural, but more generally one can select arbitrary phases θ_1 and θ_2 associated with winding around the x-direction and p-direction, respectively. The pair (θ_1, θ_2) can also be seen as fixing (quantizing) the locations of the finitely many ($N = 1/h$) p-states and x-states, respectively, on the unit square. Physically, one can imagine varying boundary conditions by changing the (shielded) magnetic flux through a circle on which an electrically charged particle is constrained to move. One thus obtains an infinite set of quantizations, all having the same semiclassical limit.

The kinematics on a torus is given by a basis of N position states $|i\rangle$, $i = 0..N-1$, with positions $x(i) = (i + \theta_2)/N$, and a momentum basis $|\tilde{j}\rangle$, $p(\tilde{j}) = (\tilde{j} + \theta_1)/N$ related to this by a discrete Fourier transform. We will be interested in the properties of eigenstates of this system in the momentum basis, which is the eigenbasis in the $a \rightarrow 0$ limit.

First the classical properties of this system need to be discussed. An important property, which it shares with the titled billiard described earlier is the logarithmically slow spreading in momentum space. Classically, the momentum jumps up or down by a (mod 1) on every iteration, but, as in the case of the tilted billiard, the long-time behavior does not resemble a random walk, but rather is logarithmic, in accordance with Equation (15). The numerical values are $m_T = 1.9 + 0.85 \log(T)$ and $n_T = 1.8 + 1.2 \log(T)$. In obtaining these values, an ensemble average over kick strength a and kicking periodicity b is performed, as well as an averaging over the starting point. Very similar behavior is obtained fixing $b = 1$ (in which case the kinetic term is continuous). In this case the numerical results are $m_T = 1.55 + 0.85 \log(T)$ and $n_T = 1.7 + 0.95 \log(T)$. The logarithmic behavior persists to times as long as $T = 10^7$ iterations, as shown in Fig. (7).

FIG. 7. Logarithmic classical spreading in momentum for kicked sawtooth map, Eq. (15).

⁶Classically, this system is very similar to a particle bouncing back and forth in a hard-wall one-dimensional box, with periodic kicks of fixed impulse directed towards the right side of the box.

⁷Compactifying the x variable on $[0, 1]$ is natural given that the potential is already periodic. It then makes most sense to compactify p on the interval $[0, 1/b]$, in which case without loss of generality $b = 1$. We may also retain b as a free parameter while compactifying p on the interval $[0, 1]$, resulting in a discontinuous kinetic term. Fixing b or allowing it to vary has no qualitative impact on the quantum results.

Diffracton has a similar effect here as in the tilted billiard system, causing $N < P(a|a) >$ to grow only as $\sqrt{N}/\log(N)$ instead of the semiclassically predicted $N/\log(N)$ behavior, while $N^2 < P(a|b)^2 >$ is generic (independent of N). Here averaging is performed over boundary conditions $\theta_{1,2}$ as well as over the classical kick strength a described above (kick periodicity b is fixed at 1). Specifically, the numerical results we obtain are $N < P(a|a) > = 2.5\sqrt{N}/\log(2N)$ for N in the range 100 to 1000, while $N^2 < P(a|b)^2 >$ remains constant around 1.55 in the same range. The power-law scaling of the diffracton pattern, in accordance with Eq. (16), is shown in Fig. (10), for a classically nonergodic version of this system, with a rational kick strength $a = 1/3$. (Using a rational kick strength allows us to look at diffractive behavior in isolation, in the absence of long-time classical spreading.)

FIG. 8. Iterations of the propagator (absolute value) and the $P(a|b)$ matrix, for kicked sawtooth map.

FIG. 9. Inverse participation ratio, Eq. (17), for kicked sawtooth map.

This behavior is interesting in connection with the limits discussed earlier given by Equation (14), where we saw that single-state transport can remain generic as long as $N < P(a|a) >$ grows no faster than \sqrt{N} . In both of the systems studied here, diffracton alone limits $N < P(a|a) >$ to be within this bound. This may suggest that non-classical effects are always sufficient to give ergodic transport, no matter how slow the classical spreading may be.

FIG. 10. Log of the power-law diffracton statistics for nonergodic kicked sawtooth map, Eq. (16). The peaks are fit to the form $\log[0.01/\sqrt{n-j}]$, where j is the position of each peak maximum.

VII. CONCLUSION

The possible types of quantum ergodicity we have discussed are schematized in Fig. (11). Starting with the (impossible in general) strict quantum ergodicity, we show RMT with its χ^2 distributed p_n^a 's, followed by two types of weak quantum ergodicity. These two differ as to whether only $< P(a|a) >$ is anomalous (Weak I) or whether $< P(a|b)^2 >$ is also anomalous (Weak II). All these fall within SCdVZ ergodicity; only the last, localized case does not. The examples presented here are both in the Weak I category.

We have seen that in classically ergodic systems where the classical rate of spreading is sufficiently slow, quantum mechanics is only able to take advantage of that classical phase space exploration which occurs before the Heisenberg time (i.e. before the time at which individual eigenstates are resolved). This gives rise to a previously unexplored localization phenomenon in such systems, involving a growing deviation from random matrix theory predictions as the classical limit $h \rightarrow 0$ is taken. Because of the non-commutativity of the $h \rightarrow 0$ and $T \rightarrow \infty$ limits, we obtain a situation in which quantum eigenstates become less and less ergodic even as the quantum mechanics follows the (ergodic) classical mechanics for longer and longer times. Importantly, there is nonetheless no disagreement with the prior results of Schnirelman [13], Colin de Verdiere [14], and Zelditch [15] concerning ergodicity of eigenfunctions.

These “slow ergodic” systems also give rise to an interesting interplay between classical and hard quantum (diffractive) phase space exploration. The pattern of quantum transport can be well understood by superimposing diffractive spreading on top of classically allowed motion. This provides a new laboratory for examining the strengths and limitations of semiclassical methods, and for separating out classically-based and classically-forbidden quantum effects.

The “tilted billiard” and “kicked sawtooth potential” systems discussed in this paper are part of a diverse spectrum of classical systems and their quantum counterparts. This spectrum includes (1) integrable systems, (2) nonergodic systems such as rational-angle polygonal billiards, (3) “slow ergodic” systems, (4) ergodic systems with zero Lyapunov exponents (generic polygonal billiards), (5) mixed systems, and (6) chaotic (i.e. mixing) systems. Different time scales and different issues of quantum-classical correspondence arise in each of these situations. Furthermore, transitions between many of the regimes given above can be obtained by varying \hbar for a given classical system.

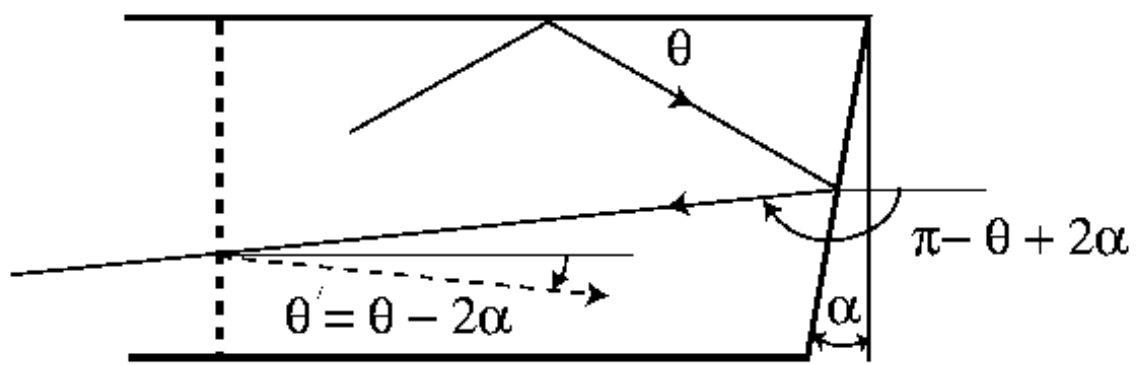
In all of these cases, an understanding of eigenstate and transport properties, as well as of spectral characteristics, is crucial for a full appreciation of the quantum-classical relationships. In this paper, we have outlined a formalism which should prove useful in many situations for studying the deviations from universality of eigenstate and transport statistics.

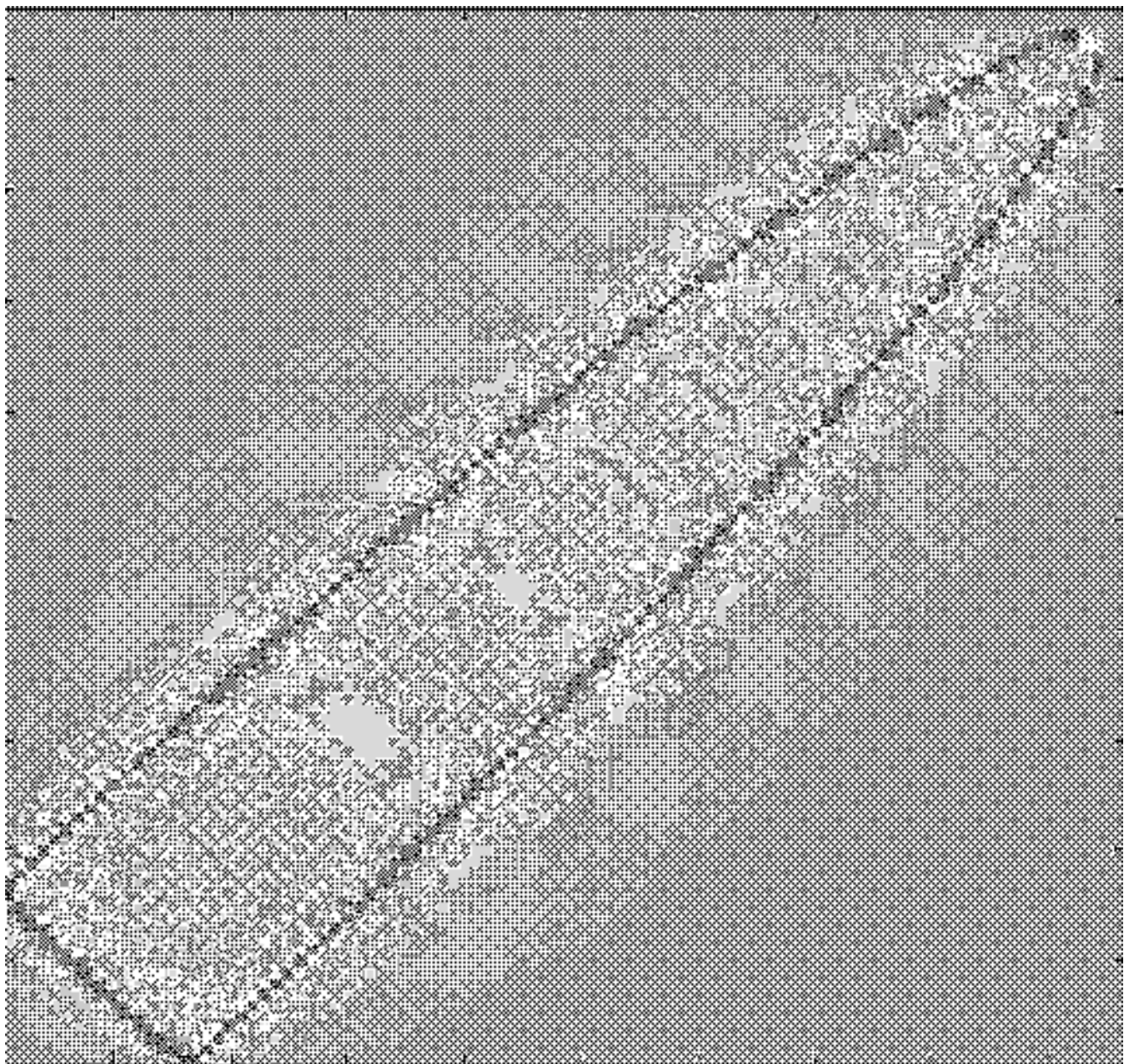
VIII. ACKNOWLEDGEMENTS

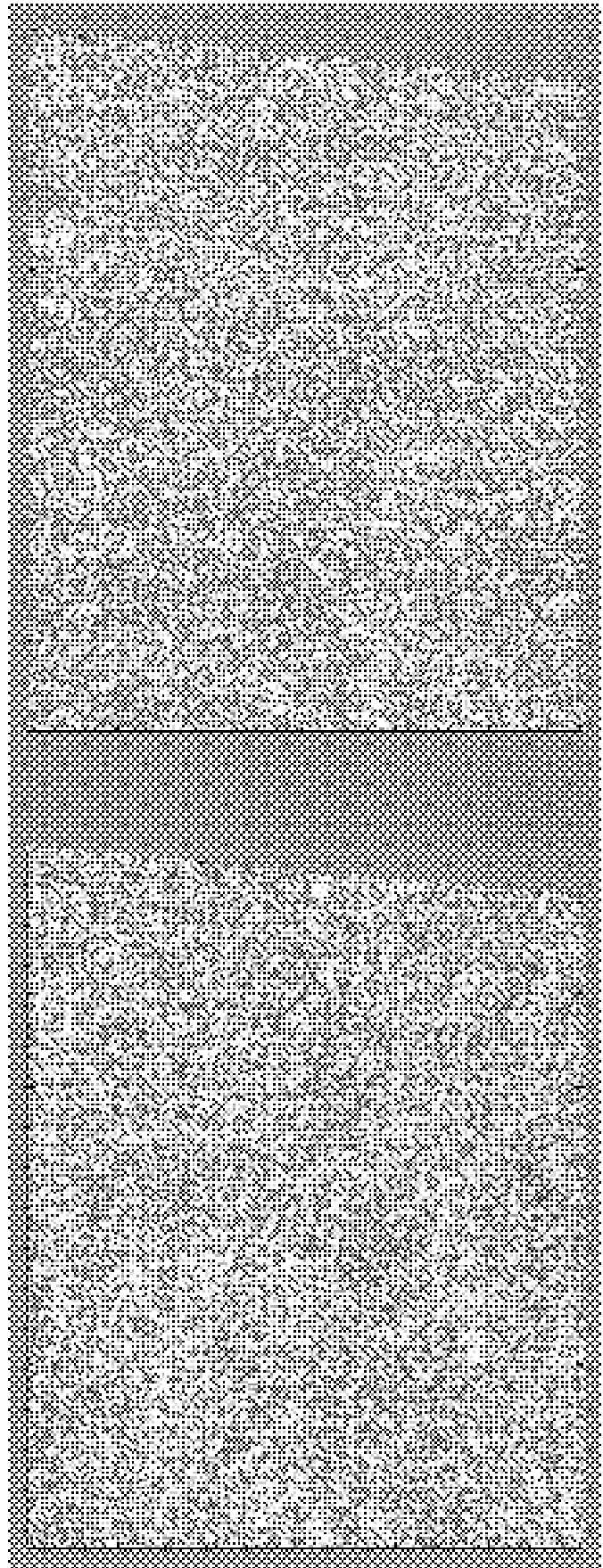
This research was supported by the Harvard Society of Fellows and by the National Science Foundation under grant number CHE-9014555.

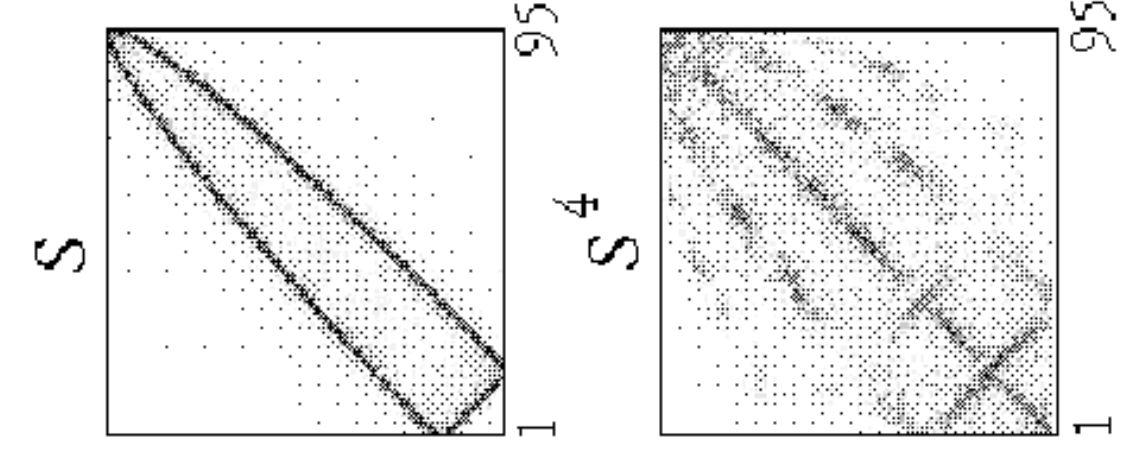
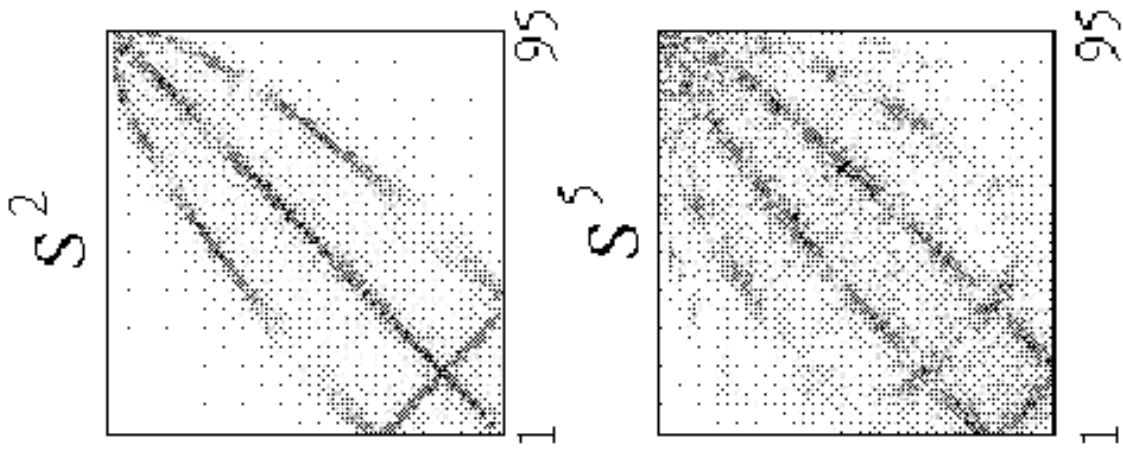
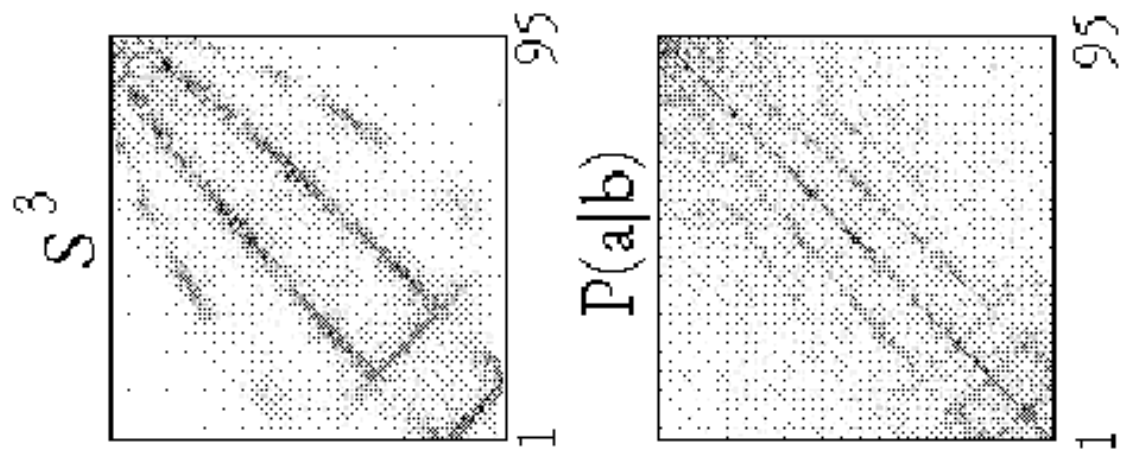
FIG. 11. Schematic of the possible types of quantum ergodicity, as shown through the qualitative behavior of p_n^a and $P(a|b)$. The first four are consistent with SCdVZ theorem, the last is simply shown for contrast to illustrate a nonergodic case.

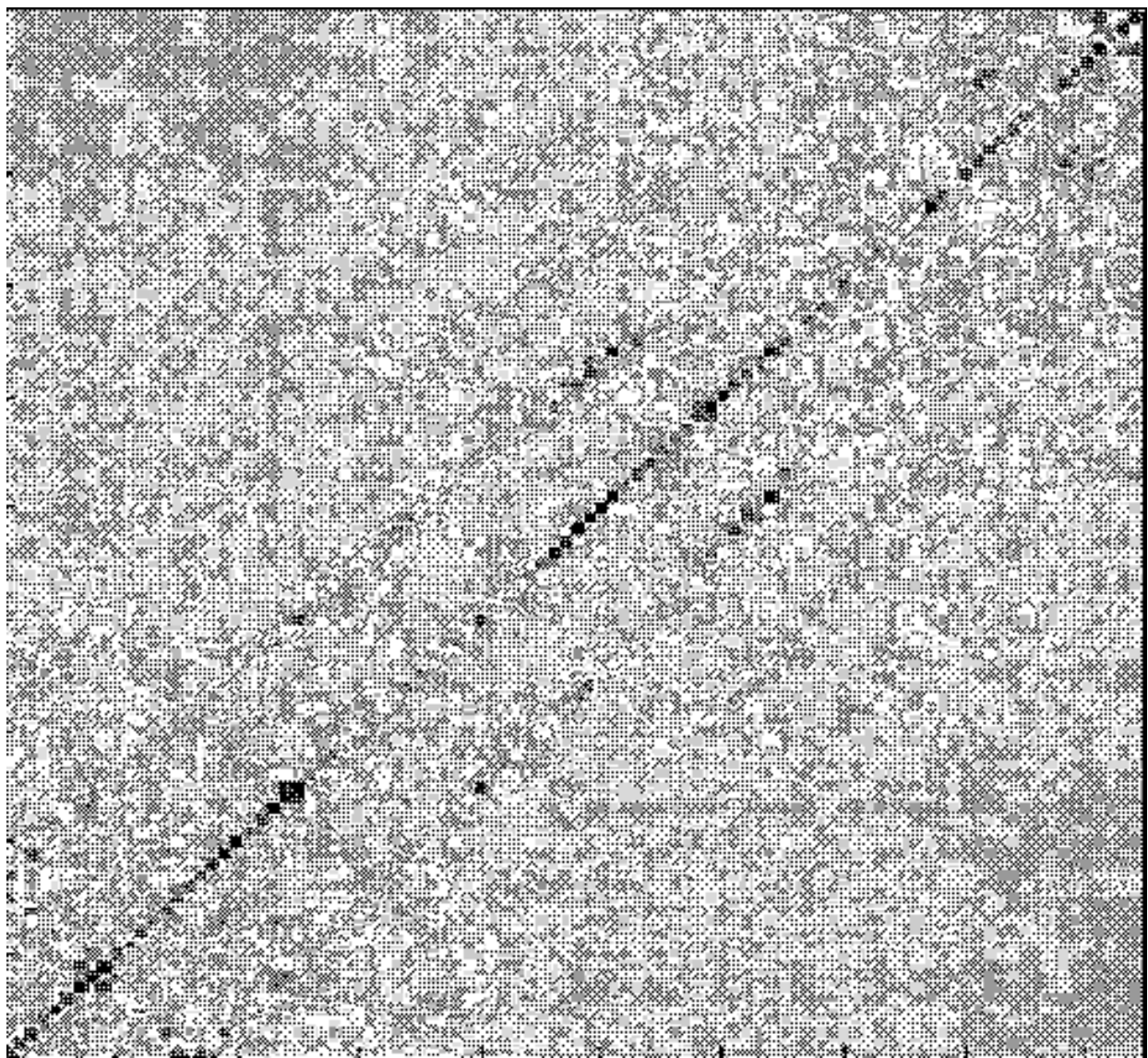
- [1] M. V. Berry, in *Chaotic Behaviour of Deterministic Systems*, ed. by G. Iooss, R. Helleman, and R. Stora (North-Holland 1983) p. 171.
- [2] O. Bohigas, M.-J. Giannoni, and C. Schmit, *J. Physique Lett.* **45**, L-1015 (1984).
- [3] See, e.g. M.L. Mehta, *Random Matrices*, Academic Press (1991); T. A. Brody, J. Flores, J. B. French, P. A. Mello, A. Pandey, and S. S. M. Wong, *Rev. Mod. Phys.* **53**, 385 (1981).
- [4] E. J. Heller and R. L. Sundberg, in *Chaotic Behavior in Quantum Systems*, G. Casati, ed. (Plenum 1985) p. 255.
- [5] S. Tomsovic and E. J. Heller, *Phys. Rev. Lett.* **67**, 664 (1991); L. Kaplan and E. J. Heller, *Phys. Rev. Lett.* **76**, 1453 (1996).
- [6] P. O'Connor, J. N. Gehlen, and E. J. Heller, *Phys. Rev. Lett.* **58**, 1296 (1987).
- [7] E. J. Heller, *Phys. Rev. Lett.* **53**, 1515 (1984).
- [8] E. B. Bogomolny, *Physica* **D31**, 169 (1988).
- [9] M. V. Berry, Les Houches Lecture Notes, Summer School on Chaos and Quantum Physics, M-J. Giannoni, A. Voros, and J. Zinn-Justin, eds., Elsevier Science Publishers B.V. (1991); M.V. Berry, *Proc. Roy. Soc. A* **243**, 219 (1989).
- [10] S. Tomsovic and E. J. Heller, *Phys. Rev. Lett.* **70**, 1405 (1993).
- [11] L. Kaplan and E. J. Heller, to be published.
- [12] M. V. Berry, *Proc. Roy. Soc. A* **400**, 229 (1985).
- [13] A. I. Schnirelman, *Usp. Mat. Nauk.* **29**, 181 (1974).
- [14] Y. Colin de Verdiere, *Commun. Math. Phys.* **102**, 497 (1985).
- [15] S. Zelditch, *Duke Math. J.* **55**, 919 (1987); S. Zelditch and M. Zworski, *Commun. Math. Phys.* **175**, 673 (1996).
- [16] M. Degli Esposti, S. Graffi, and S. Isola, *Commun. Math. Phys.* **167**, 471 (1995); A. Bouzouina and S. de Bievre, *Commun. Math. Phys.* **178**, 83 (1996).
- [17] P. W. O'Connor and E. J. Heller, *Phys. Rev. Lett.* **61**, 2288 (1989).
- [18] E. J. Heller, *J. Chem. Phys.* **72**, 1337 (1980); E. J. Heller and M. J. Davis, *J. Phys. Chem.* **86**, 2118 (1982); E. B. Stechel and E. J. Heller, *Ann. Rev. Phys. Chem.* **35**, 563 (1984); E. J. Heller, *Phys. Rev. A* **35**, 1360 (1987).
- [19] H. Schanz and U. Smilansky, *Chaos, Solitons, and Fractals* **5**, 1289 (1995).
- [20] E. Bogomolny, *Chaos* **2**, 5 (1992).

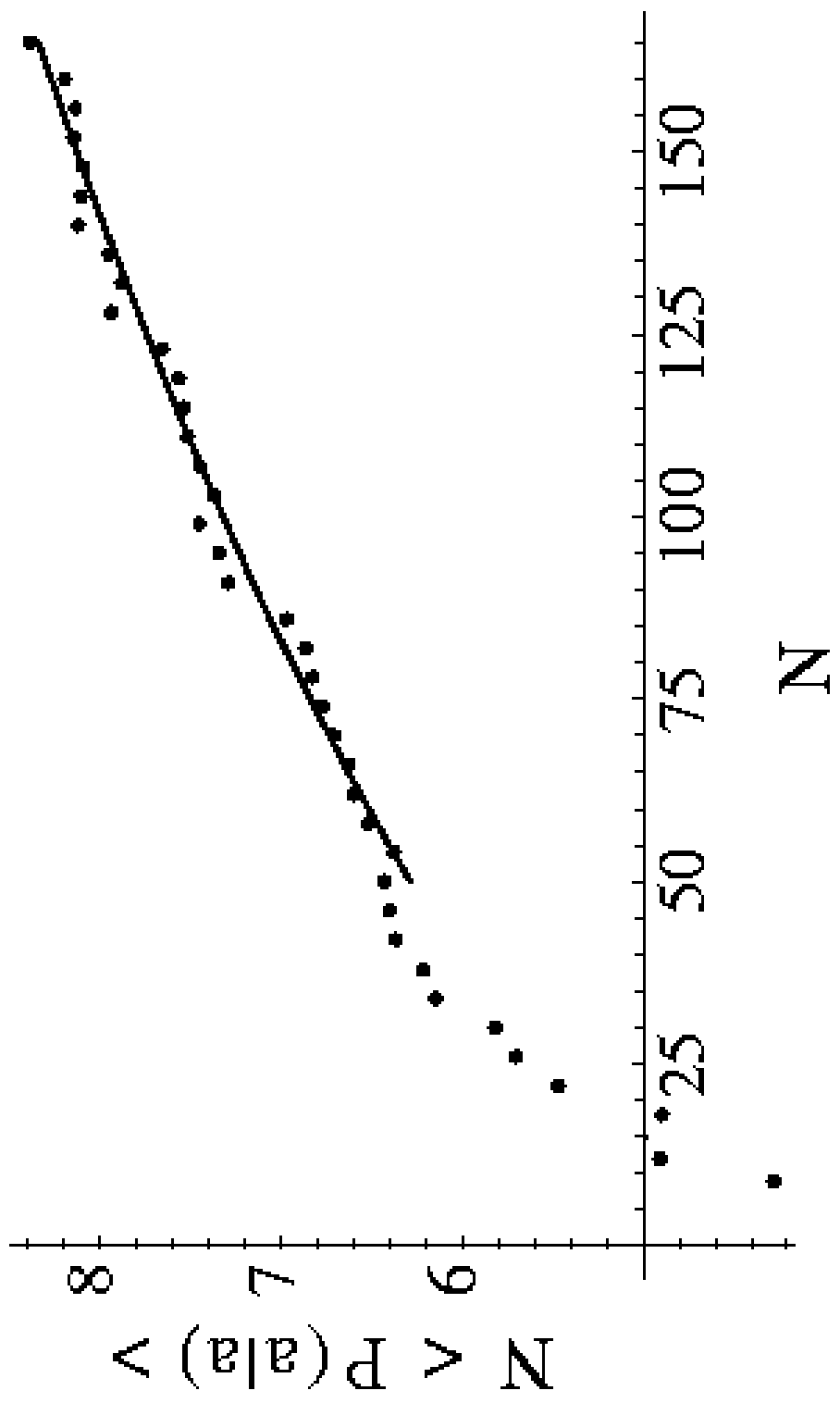


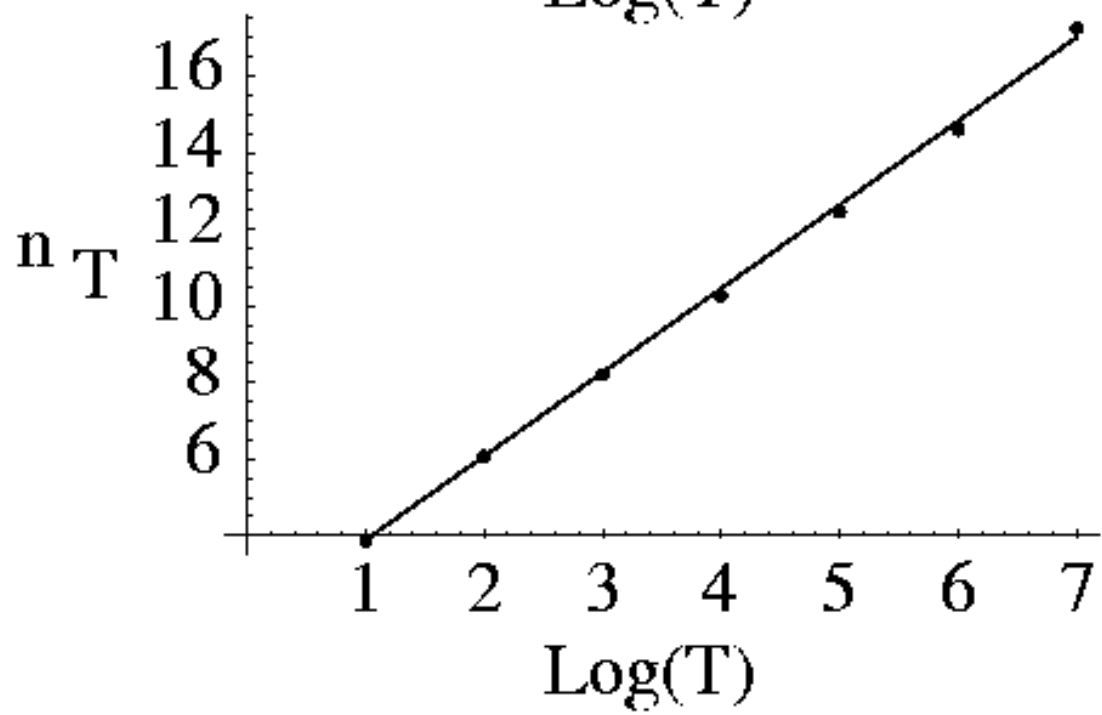
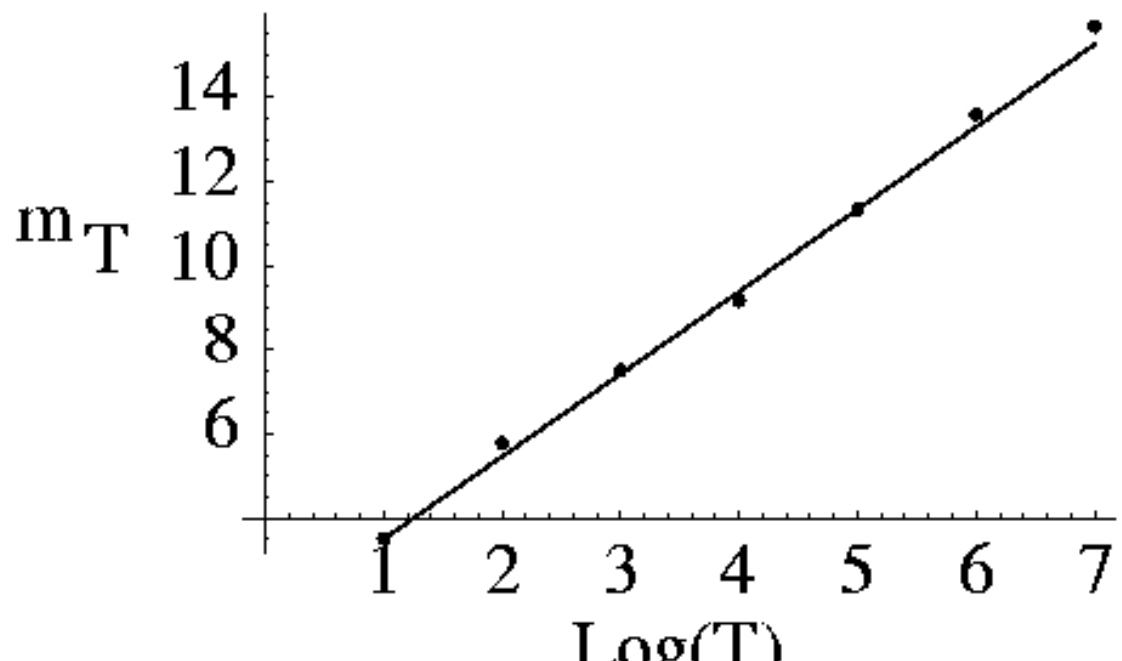


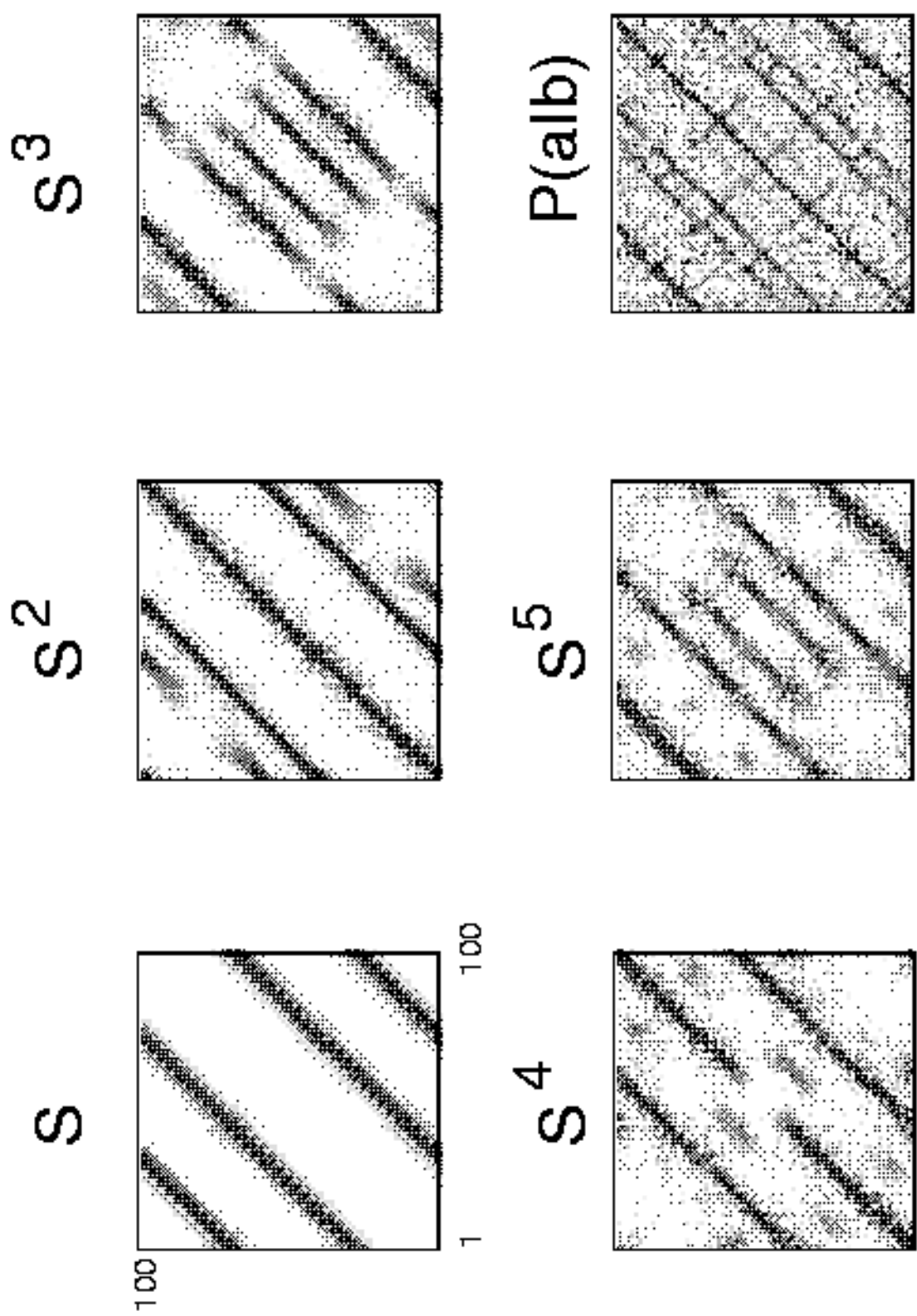


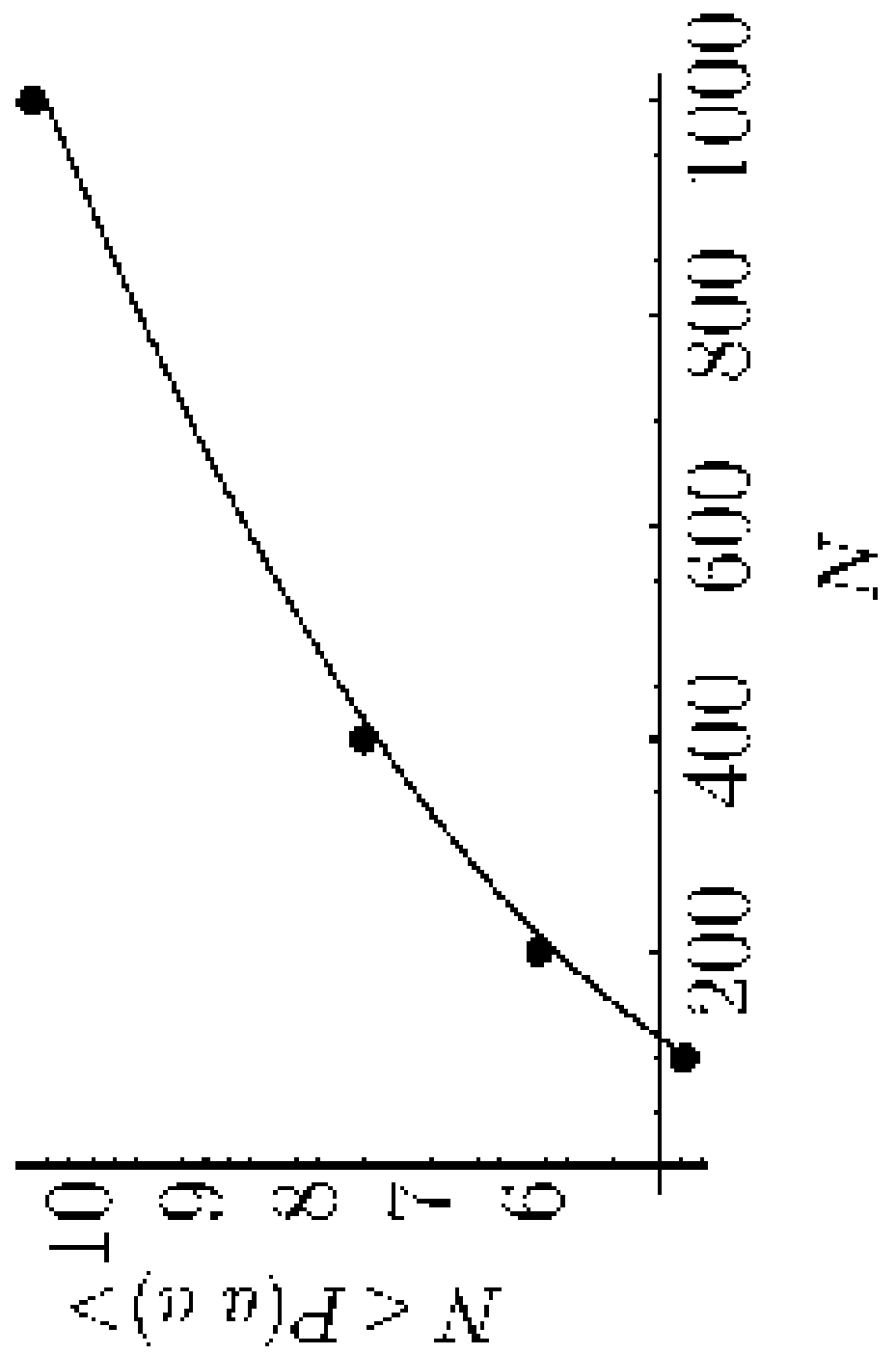


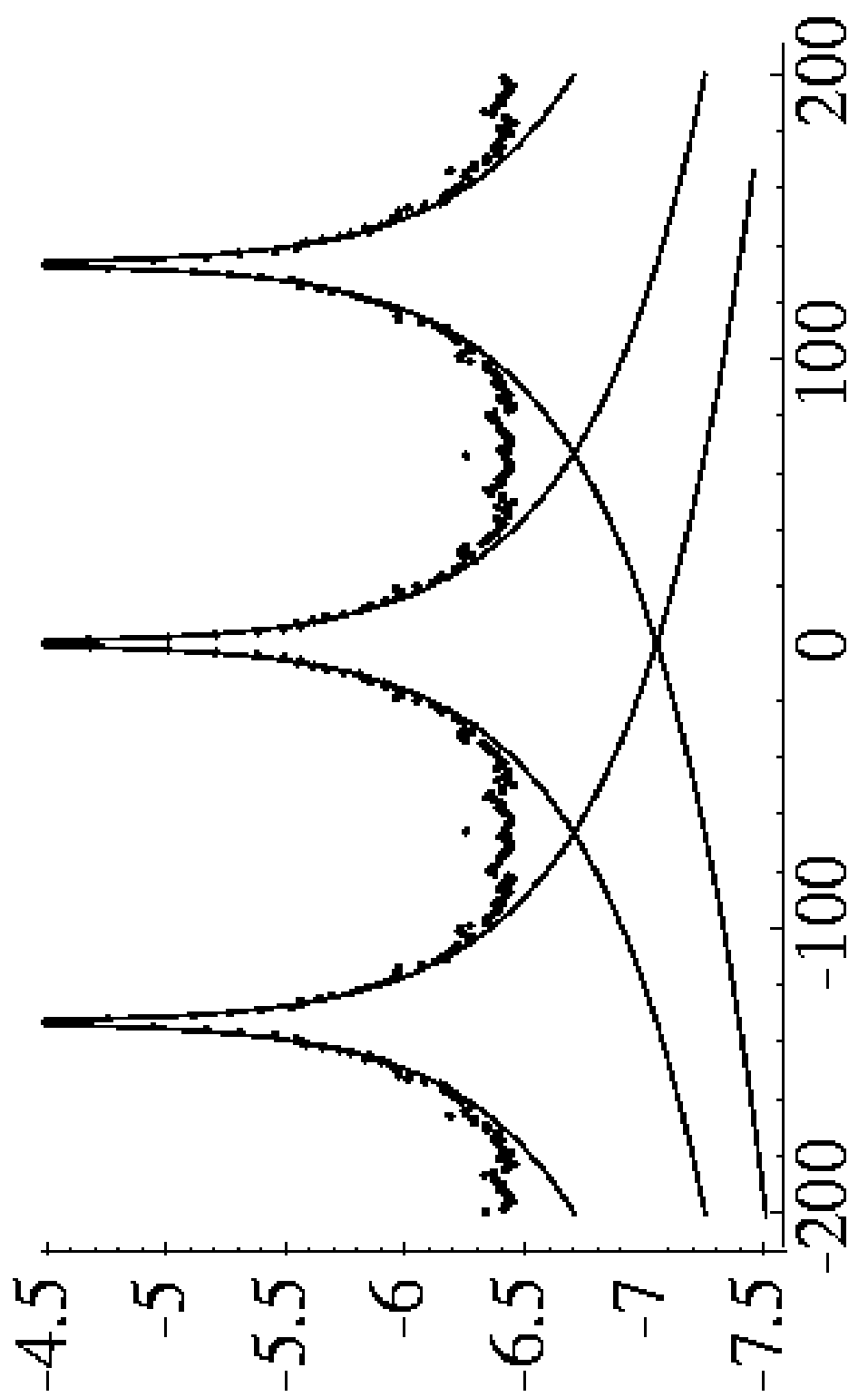






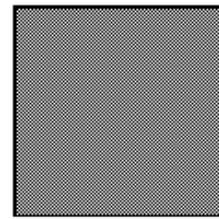
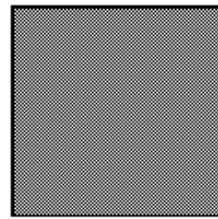




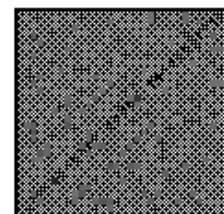


p_n^a $P(a|b)$

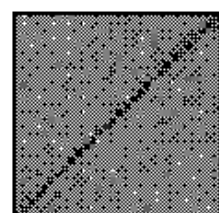
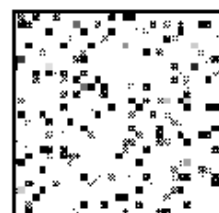
Strict
(uniform)



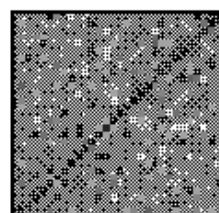
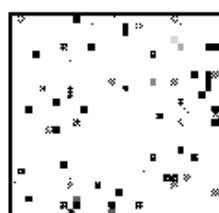
Strong
(gaussian)



Weak I
(anomalous
 $\langle P(ala) \rangle$)



Weak II
(anomalous
 $\langle P(alb) \rangle^2$)



Nonergodic
(localized)

